Experimental investigation on vibration sensitivity of an indoor glass footbridge to walking conditions

Chiara Bedon

University of Trieste, Department of Engineering and Architecture, Piazzale Europa 1, Trieste, 34127, Italy

ARTICLE INFO

Keywords:
Laminated glass
Pedestrian suspension glass structure
Field vibration experiments
Dynamic properties
Human-structure interaction (HSI)
Human comfort

ABSTRACT

For decades, the vibration performance of pedestrian structures, like footbridges and floors, has attracted the attention of researchers. According to the literature, specific vibration performances must be satisfied, depending on the class of use, structural typology and material composition of a given pedestrian system. Additional design issues, however, may derive from the presence of structural components that can be susceptible to unfavourable ambient conditions and/or time or extreme loads, including progressive degradation of material properties. This is the case for glass structures, where mostly slender load-bearing elements (with high span-to-thickness ratio) are used in combination with complementary materials (i.e., for bonding) that are often characterized by time/temperature/ambient-dependent behaviour. The relatively high span-to-thickness ratio generally manifests itself in structural masses that can be small, compared to the occupants. Human-Structure Interaction (HSI) phenomena, in this regard, may be relevant and require dedicated studies. In this paper, the dynamic performance of an existing indoor suspension glass footbridge is taken into account and explored via Operational Modal Analysis (OMA) techniques. A wide range of loading configurations (i.e., walking scenarios) are of technical interest and thus taken into account for the case-study system. These include variations in the imposed human-induced vibrations, such as the movement features, number of occupants (combined standing/walking persons), ambient conditions, size effects and mechanical restraints. Sensitivity of measured accelerations, fundamental frequencies and damping ratios for the occupied system is then discussed.

1. Introduction

In modern buildings, structural glass is recognized to act as a constructional material with load-bearing capacities, in the form of columns, beams, plates, and even complex systems. Several research studies have been spent to investigate a multitude of aspects, to support the development/refinement of enhanced design methods and optimized structural use of materials [1–5]. The vulnerability of glass structures, in this regard, is implicitly related to the material properties and on the structural typology object of design [6,7]. This is also the case of complex systems and/or pedestrian glass assemblies, where – even under ordinary operational conditions – rigid design assumptions should be taken into account, to avoid potential consequences for pedestrians, in case of accidental/extreme events [8–13], or satisfactory structural performances but still limited in-service comfort levels for the occupants. Such a category of glass structures includes indoor/outdoor slabs and footbridges (i.e. [14–16] and Fig. 1), or monumental stairs [17,18], that are built in a multitude of design details and typologies (i.e., with different joints, adhesive bonds or mechanical connections). In addition to "conventional" stress/deflection design requirements [6,7], excessive or uncomfortable vibrations may in fact require specific interventions, at the design stage but especially during the life-time of a given glass system.

The expected dynamic performance can be in fact affected by several parameters, like loading features, structural geometry, bonding layers and/or mechanical restraints that could manifest time/temperature/humidity-varying properties [19,20]. In the context of vibration serviceability, these effects could manifest in the progressive variation of boundary conditions, and/or even marked modification of the inertial properties for the resisting cross-section in use. Additional issues in dynamic conditions could be then enforced by Human-Structure Interaction (HSI) phenomena, that conventionally represent a set of continuous, mutual dynamic effects of humans and a given structure, on each other. According to several literature efforts, the time-varying forces due to walking pedestrians on a flat surface are typically expected to manifest in three directions (i.e., vertical, horizontal-lateral and horizontal-longitudinal) that could result in critical structural performances [21]. As far as vertical vibrations are more pronounced for a

E-mail address: chiara.bedon@dia.units.it.

Fig. 1. Example of glass footbridge in Rotterdam (NL, Copyright © HG Esch).

given pedestrian system, see Section 2, the typical human body can be thus intended as a Single Degree of Freedom (SDOF) system with own mass, stiffness, damping parameters and a certain walking frequency. The corresponding HSI effects can consequently change, based on a combination of structural properties (boundaries, materials, etc.) and human body movements (position, type of activity, etc.), hence requiring advanced calculation methods and the support of field experiments/Finite Element (FE) numerical simulations [21–26]. Even more attention could be required for pedestrian glass systems, due to their intrinsic mechanical and geometrical properties (compared to traditional constructional materials and typologies), and thus sensitivity to common walking scenarios.

In this paper, experimental studies and Operational Modal Analysis (OMA) techniques are dedicated to an existing indoor glass footbridge in Italy (Section 3). Based on a wide range of test configurations of technical interest, the sensitivity of dynamic estimates (i.e., acceleration peaks, fundamental frequency and damping) is experimentally assessed for the occupied structure, with respect to several key parameters (i.e., walking features, number of occupants, ambient conditions). The research study herein presented follows and extends the dynamic investigation summarized in Ref. [16]. Compared to Ref. [16], where a selected portion of the empty structure was experimentally characterized in the dynamic field, the attention of this paper is focused on HSI effects. In addition, taking advantage of FE studies (ABAQUS [27]) and dynamic formulations [28], the experimental study is herein extended to two different footbridge portions having specific behaviours, dynamic properties, and thus sensitivity to the imposed pedestrian loads.

2. Glass structures and vibrations

2.1. Safety design requirements for pedestrian glass structures

Structural glass floors and pedestrian systems are designed to satisfy rigid performance requirements under ordinary service loads, namely related to maximum deformations (Service Limit State – SLS) and stresses (Ultimate Limit State – ULS), see Refs. [1,6,7]. For conventional loading/boundary configurations, the cumulative deflection u_{max} due to permanent/accidental design actions is in fact limited to a maximum value $u_{lim} = L_0/250$, while more restrictive/dedicated deflection limits should be taken into account for special structures [1,6,7]. The ULS stress peaks must then be lower than the design tensile resistance of glass, where the latter depends on a multitude of geometrical and mechanical parameters (i.e., type of glass, boundary and loading condition, time loading, edge treatments, holes). Special attention should be spent for stress peaks in compression, depending on the loading/boundary condition. Finally, a key design step is represented by the verification of the post-cracked residual resistance, stiffness and redundancy that the (eventually damaged) glass system should satisfy at the Collapse Limit State (CLS). Such a series of design checks, see Refs. [1,6,7], can be generally satisfied based on an optimal combination of glass types, layers (i.e., minimum three for pedestrian systems) and boundaries (with four side linear supports to privilege). For conventional systems, simplified equivalent thickness approaches can also offer reliable estimates for design (i.e. [29]).

2.2. Vibration serviceability

While several calculation methods and design recommendations are available for the design and assessment of glass members/structures with respect to expected deformations and stress peaks/distributions, the dynamic vibration response is a relatively recent research topic. Most of the existing studies, see Refs. [30–35], include experimental, analytical and numerical analyses devoted to exploring the dynamic behaviour of simple glass members, even in presence of flexible restraints/bonding layers with viscoelastic phenomena. Even more attention should be spent for pedestrian glass structures, given the common use of glass in wide surfaces for floors and roofs [36–40].

However, major practical limits are frequently represented by the lack of appropriate knowledge and/or calculation instruments that could be extended from other pedestrian systems to structural glass solutions [41].

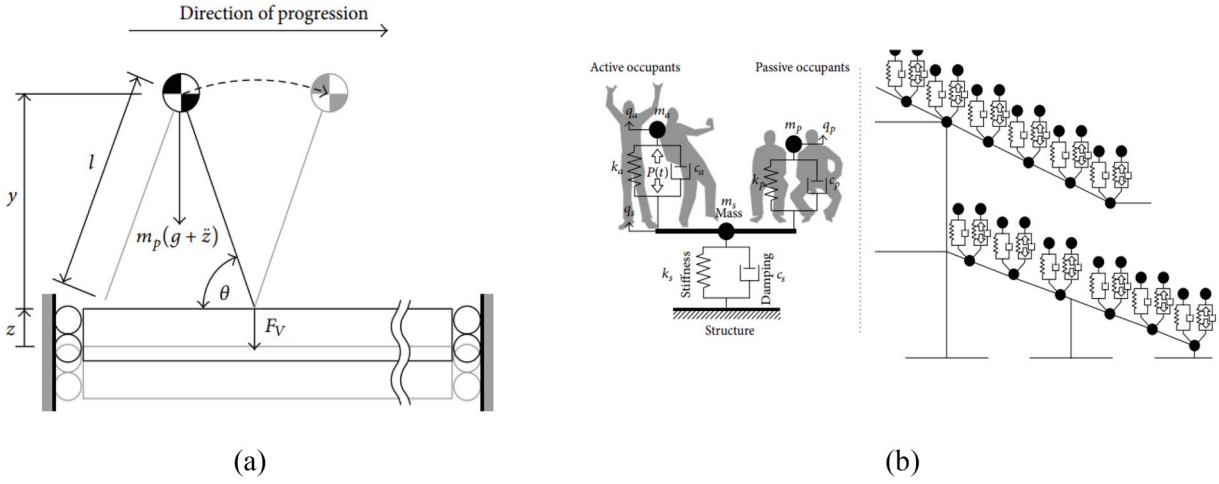

Fig. 2. Mathematical models for HSI calculations of pedestrian structures: (a) inverted pendulum approach, according to Ref. [25], and (b) crowd effects estimates on stadium structures [49]. Both figures reproduced from Ref. [21] under the terms and condition of a CC BY-NC 4.0 license.

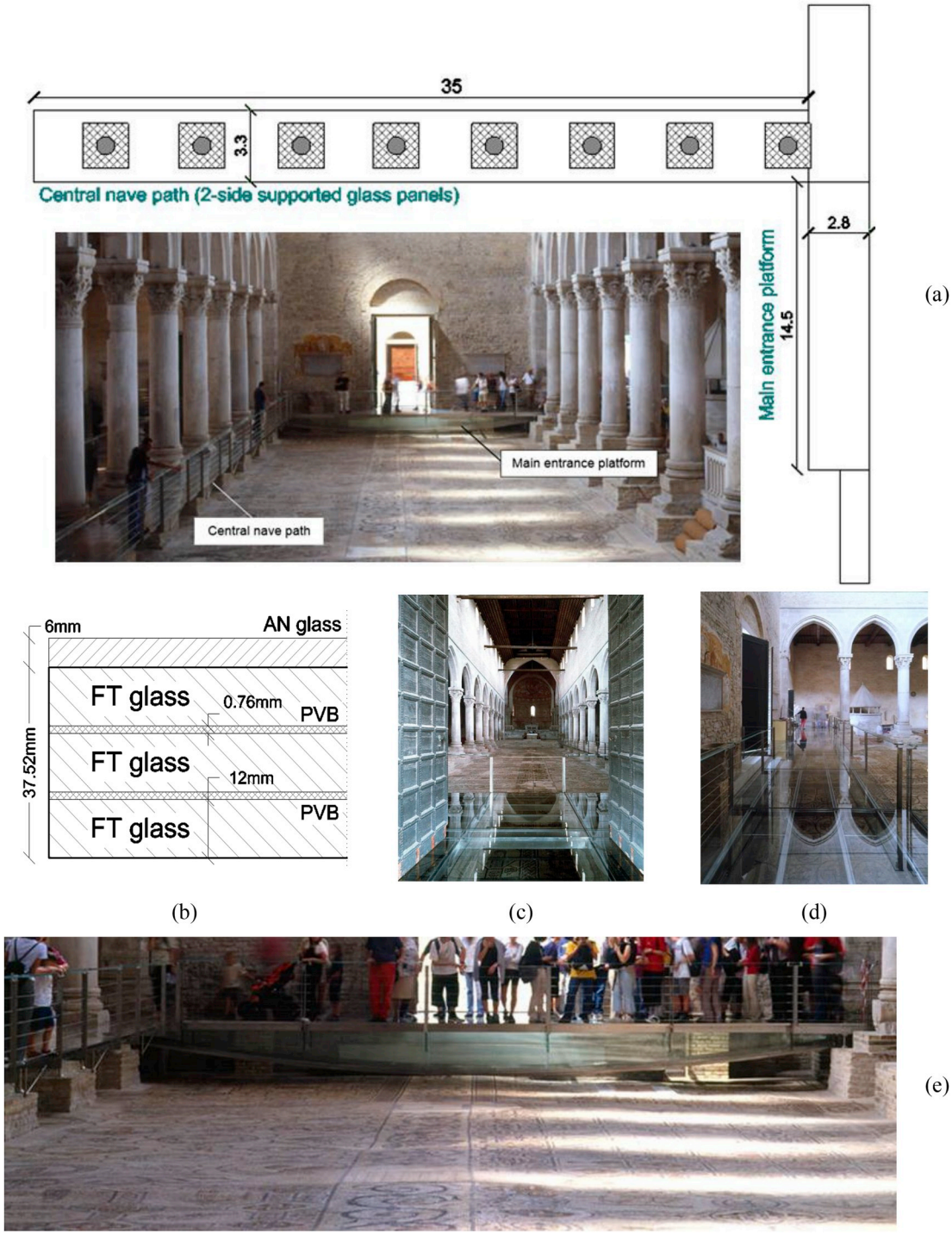

Fig. 3. Case-study pedestrian system: (a) top schematic view (global dimensions in meters) and (b) nominal cross-sectional details of the glass slab, with (c)-(d)-(e) general views of the in-service structure (photos reproduced with permission from So.Co.Ba).

As a general rule, glass slabs should be verified in operational conditions in the same way of pedestrian structures composed of traditional constructional materials. This is also the case of glass stairs, where even more restrictive vibrational performance levels are required (see for example [42]).

Based on ISO 2631–2: 2003 provisions [43], for example, the "optimal" vibration condition for pedestrian systems can be considered satisfied as far as the vertical fundamental frequency f_1 of a given slab is at least equal to 8 Hz, while advanced calculation approaches/different limit conditions are recommended for the analysis of structural systems with relatively low frequency or specific typology and class of use [44–46]. Possible critical aspects of glass pedestrian structures, in this regard, can be represented by typically high span-to-thickness ratio for slabs, with intrinsic flexibility and slenderness that are generally maximized, compared to other traditional slabs in buildings. Another influencing parameter is represented by the use of unconventional or limited restraints (i.e., point supports). Additional uncertainties may finally derive from the progressive degradation of restraints or local load-bearing components (i.e., Section 5), thus resulting in a possible variation of boundary conditions in the life-time of a given system to

Fig. 4. View of the typical 2-side supported panel along the central nave path: (a) top-side axonometric view, with (b)–(c) D1 and D2 details of end supports and bracing members (photos by © C. Bedon, with permission from So.Co.Ba).

analyze.

2.3. Human-Structure Interaction (HSI) phenomena

As known, a stationary human body – with respect to a given pedestrian structure – represents a dynamic system that interacts with the structure itself. The major design issue is represented by the mutual interference of the dynamic properties of both the involved parts. Accordingly, several research studies and HSI investigations can be found in the literature [45–51], for several typologies of pedestrian systems and loading configurations. In presence of moving occupants, however, HSI phenomena may result in even more complex effects to estimate [21], due to reciprocal motion forces and on the potential of the human body to change the dynamic properties of a given structure, over which they are. Key parameters for dynamic assessments are thus represented by walking features (i.e., pacing frequency and phase, walking speed, stride length) that necessarily require dedicated tools and methods for reliable analyses (see for example [21] and Fig. 2).

From a mechanical point of view, see Fig. 2, a given pedestrian structure must satisfy the well-known equation of motion:

$$M\ddot{x}(t) + C\dot{x}(t) + Kx(t) = P(t) \tag{1}$$

with M, C, K representing the modal mass, damping, stiffness matrices respectively; $P(t)$ the imposed external (periodic) force reproducing the motion of walking occupants, x(t) the vertical displacement vector.

As far as the structure is empty ("es") and its actual restraints can be reproduced by simple supports, practical formulations are generally used to estimate the expected fundamental frequency f_{es}:

$$f_{es} = \frac{1}{2\pi}\cdot\sqrt{\frac{k_{es}}{m_{es}}} = \frac{1}{2\pi}\left(\frac{\pi}{L_0}\right)^2\cdot\sqrt{\frac{EI}{\rho}} \tag{2}$$

where ρ denotes the material linear density, E the modulus of elasticity and I the second moment of area of the $B \times t$ resisting cross-section. In addition, k_{es} and m_{es} are the stiffness and mass of the empty structure. For the occupied system, it is commonly expected that the fundamental frequency f_{os} modifies and:

$$f_{os} = \frac{1}{2\pi}\cdot\sqrt{\frac{k_{os}}{m_{os}}} \neq f_{es} \tag{3}$$

with

$$\xi_{os} = \frac{c_{os}}{2\sqrt{k_{os}m_{os}}} \neq \xi_{es} \tag{4}$$

the corresponding damping (with k_{os} and m_{os} the stiffness and mass of the occupied system).

It is worth mentioning, in this context, that in most of the cases it is observed that [21]:

- standing people conventionally reduces the frequency estimates of empty systems, that is $f_{os} < f_{es}$, while
- walking occupants generally manifest in $f_{os} > f_{es}$.

Moreover, literature studies showed that:

- when the natural frequency of walking bodies f_p is less than the empty structure f_{es}, the frequency of the occupied system is expected to be $f_{os} > f_{es}$
- if $f_p > f_{es}$, otherwise, it is generally observed that $f_{os} < f_{es}$
- the effects of walking occupants are more pronounced as the number of human bodies increases;
- damping is always expected to increase for the occupied system, compared to the empty structure.

These general considerations, however, are strictly related to a series of aspects, including the mechanical features of the structure object of analysis and the role that human bodies can induce in the vibration response of a given empty system. Moreover, it was shown in Ref. [16] that laminated glass (LG) sections require careful estimates with respect of the actual bending properties (i.e., Eq. (2)), but also damping predictions can be sensitive to operational conditions.

Another key influencing parameter, compared to slabs composed of traditional constructional materials, is represented by the structural mass of glass pedestrian systems, that can be often significantly smaller than the mass of occupants, with direct effects on possible HSI phenomena. It is in fact worth mentioning that most of HSI investigations of literature have been carried out on various typologies of load-bearing footbridges and floors, but mostly made of timber, precast reinforced concrete, steel, composite or hybrid members [21,52–57]. Research studies dedicated to the vibration performance of pedestrian glass structures, on the other hand, are still limited and requiring efforts [16,58,59].

3. Pedestrian glass system object of analysis

For the experimental investigations herein summarized, the indoor glass footbridge in Aquileia (Italy) and partly analysed in Ref. [16] was taken into account, see Fig. 3. The footbridge (built in the early 2000) takes place within a Roman Age Basilica' monument, listed by UNESCO as a World Heritage Site and including the largest (and one of the best preserved) early-Christian floor mosaics (750 square meters), with more than 300,000 visitors/year.

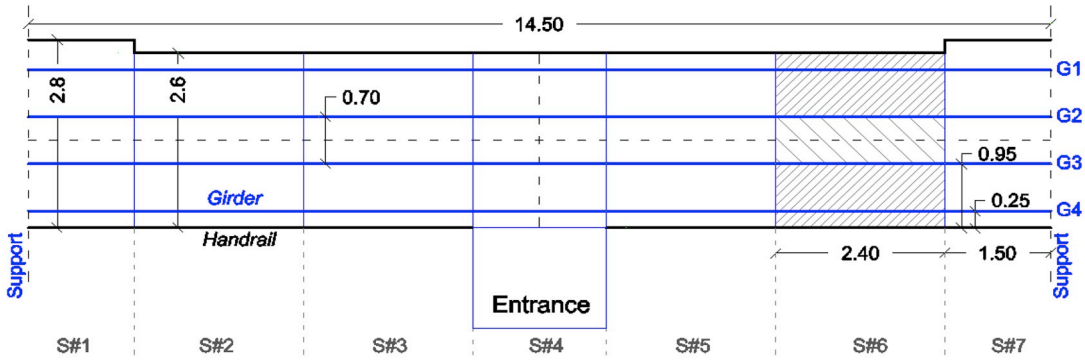

(a)

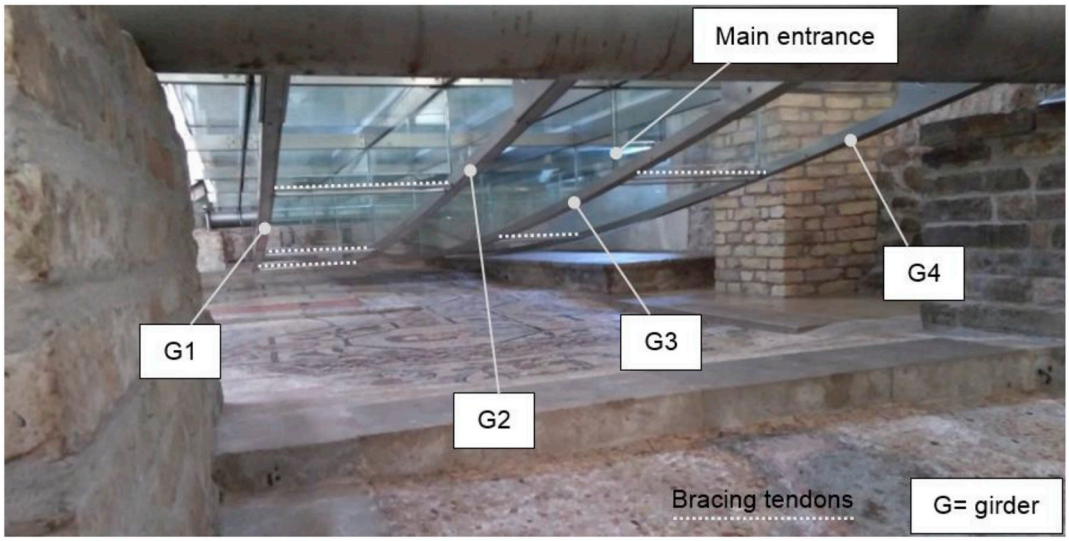

(b)

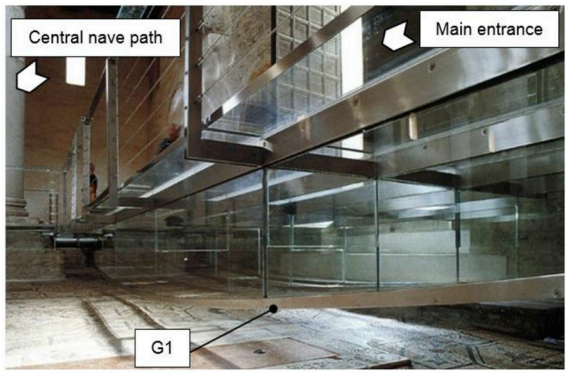

(c)

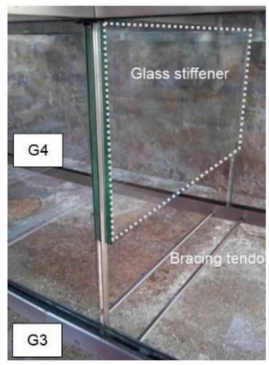

(d)

(e)

Fig. 5. Main entrance suspension platform: (a) schematic drawing (top view, all the dimensions are given in meters), with (b) bottom view; (c) front (bottom view; and (d)–(e) details of bracing system and supports (photos by © C. Bedon, with permission from So.Co.Ba).

Globally, the central nave structure object of investigation can be roughly described in the form of an unsymmetrical T-shape (Fig. 3(a)). A longitudinal path crosses the nave, via series of independent, 2-side supported glass panels (Section 3.1 and [16]), while a main entrance suspension platform allows the communication between the nave and the adjacent crypt (Section 3.2).

From a structural point of view, the overall system is characterized by the presence of a composite slab consisting of a triple LG section, see Fig. 3(b). Its nominal layout includes three 12 mm thick fully tempered (FT) glass panels, bonded via interposed PVB® foils (0.76 mm thick each). An additional annealed (AN) glass layer, 6 mm in thickness, is used to protect the LG section. According to product standards (see for example [6,7]), the nominal modulus of elasticity of glass is in the order of 70 GPa, with 0.23 the Poisson ratio and 2500 kg/m^3 the density. The key variation for FT and AN glass types in use is the substantially different tensile resistance, with 120 MPa and 45 MPa the characteristic nominal values respectively.

3.1. *Typical 2-side supported panel*

The longitudinal nave path is composed of a series of 2-side supported plates, whose vibration performance in the empty configuration has been investigated in Ref. [16]. The span of these panels is in the range from 2.5 m to 2.65 m (depending on the actual distance of columns), in order to accommodate the Basilica sub-structure (Fig. 4). Each LG plate is linearly sustained along the short edges by steel members

Table 1
Reference ambient conditions for the field experimental measurements. * = test repetitions carried out in different days.

Period	Month	Test time	Temperature [°C]		Relative Humidity [%]
			Daily (max-min)	Test (mean)	(test time)
P#1	March 2019*	9–10 a. m.	7.5/15.0	13.2	76
P#2	March 2019*	17–18 p. m.	−0.6/14.8	11.8	73
P#3	February 2019	15–16 p. m.	1.8/18.8	12.4	74
P#4	November 2017	8–10 a. m.	4.1/7.2	6.5	87

(Fig. 4(a)–(b)), while a set of steel tendon pairs (10 mm their diameter) is used to offer mid-span unilateral point supports to each slab (T1-to-T3 tendons in Fig. 4(a) and (c)). In this paper, the experimental investigations are reported for the 2-side supported plate that was selected in Ref. [16], being characterized by maximum span (2.65 m, with 1.65 m the width).

3.2. Main entrance platform

Regarding the main entrance platform, (LG + AN) glass plates with the same nominal composition proposed Fig. 3(b) are used. In this case, however, the panels are linearly supported along four sides, by a continuous metal grid composed of C-shaped steel frame members (Fig. 5(a)). The overall entrance platform covers a surface of 14.5 m × 2.8 m, that can be divided longitudinally in seven sectors (see the labels S#*n* in Fig. 5(a)). In the width of the platform, each sector is composed of three adjacent plates. The central one (2.4 m × 0.7 m) is linearly supported along the four edges. The two external plates (2.4 m × 0.95 m) are also linearly supported along three edges. The fourth linear support, in the longitudinal direction, is unsymmetrical and restrain results in a 0.25 m wide cantilever arm (Fig. 5(a) and (c)). The overall slab system is then sustained by four longitudinal steel-glass girders, spanning over the full bending length of 14.5 m (Fig. 5(b)).

The global behaviour of the entrance platform can be described – for preliminary estimates – in the form of a composite slab with end supports and beam-like response under the action of dead loads and occupants. Additional uncertainties are represented by the mechanical interaction between all the glass and steel structural components in use. OMA techniques, in this regard, are specifically recommended for structural assessment purposes.

The longitudinal girders sustaining the slab are characterized by an overall parabolic shape, and intended to act as reinforced glass beams

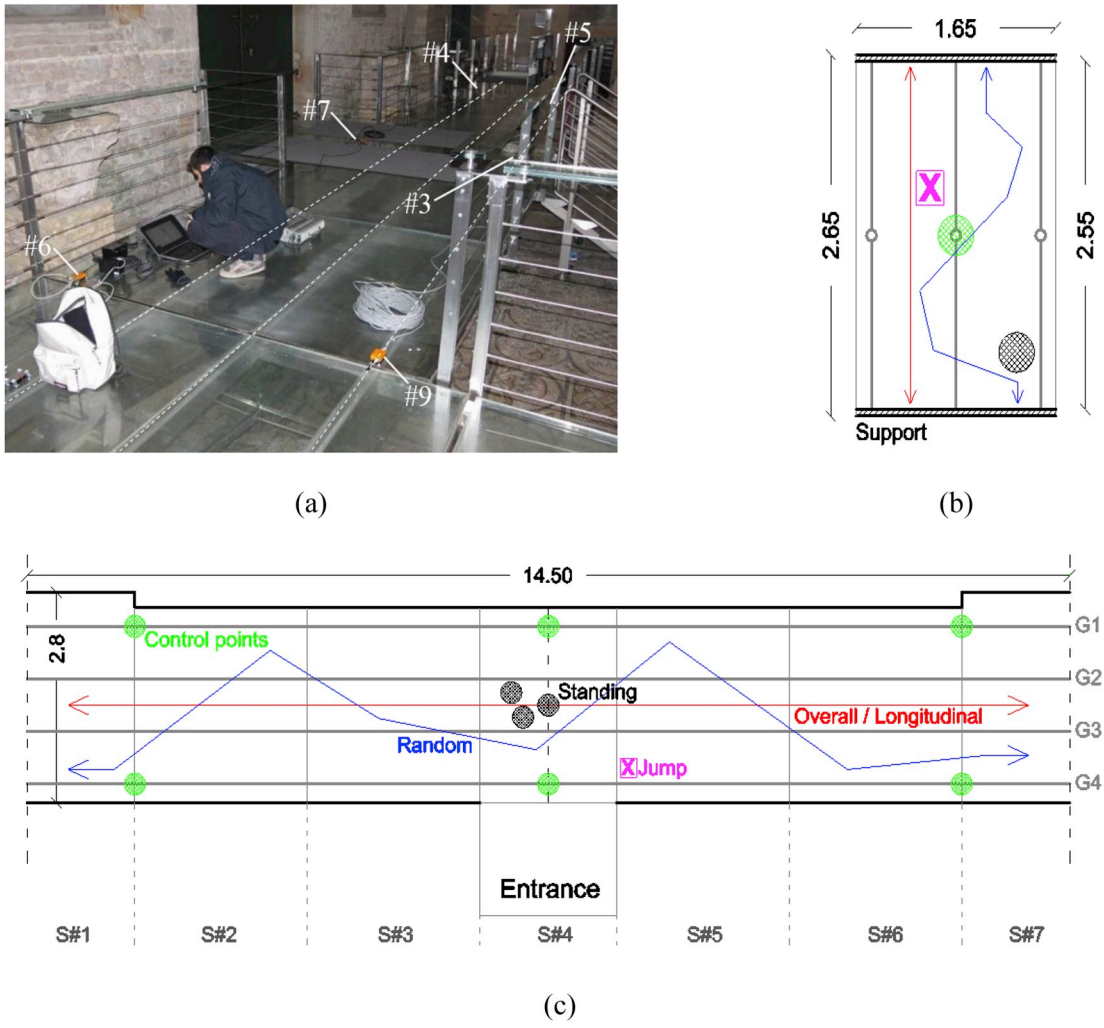

Fig. 6. (a) Typical setup for the field vibration experiments (photo by © C. Bedon, with permission from So.Co.Ba), with schematic view of selected configurations for (b) 2-side supported LG panel and (c) main entrance platform (all the dimensions are given in meters).

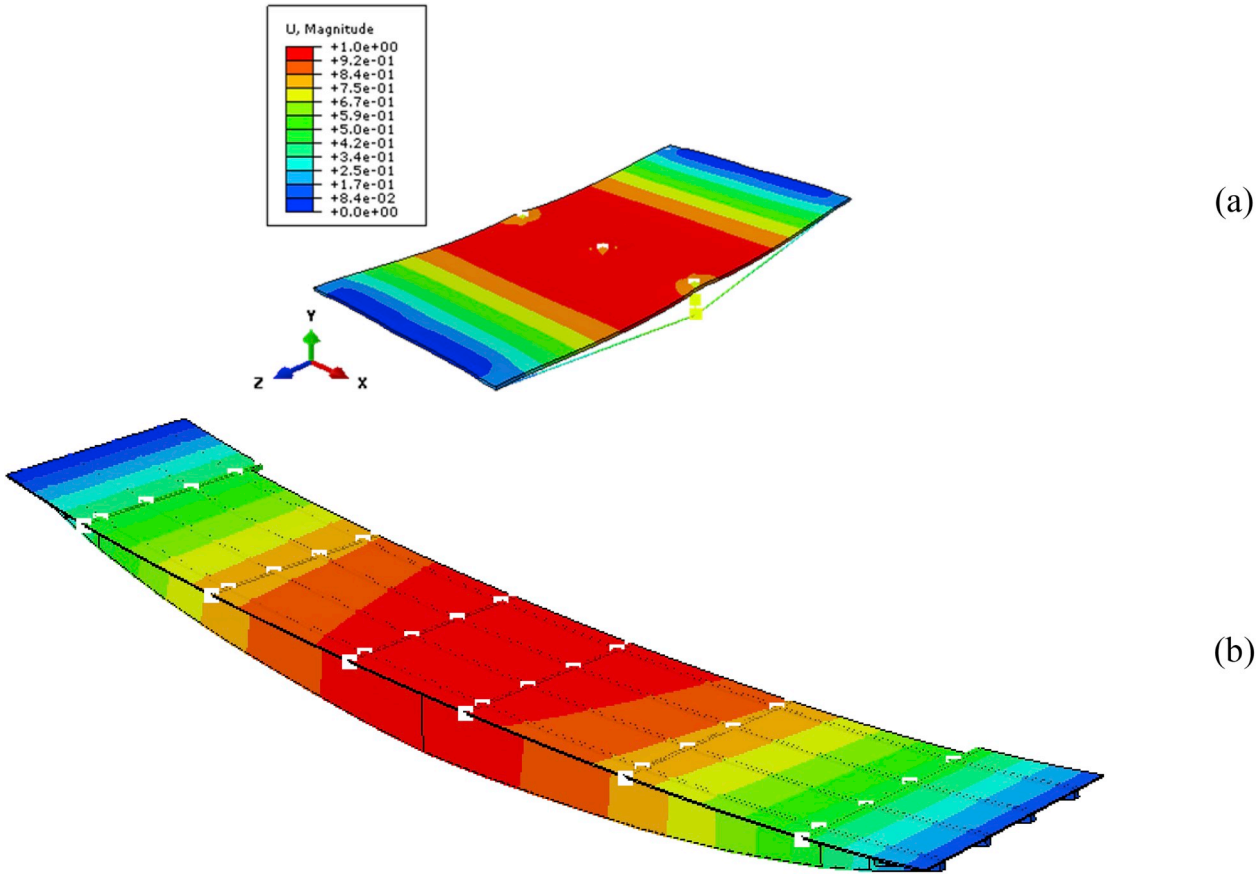

Fig. 7. Fundamental vibration shape for the (a) 2-side supported panel (according to Ref. [16]) and (b) main entrance platform (ABAQUS). In evidence, the contour plot of modal displacements (empty configuration).

offering an appropriate bracing contribution to the platform. Each girder consists of a series of segmented FT glass panels that are used in combination with continuous steel members, see Fig. 5(b) and (c).

In order to avoid possible lateral-torsional buckling phenomena for the slab as a whole, these girders are then restrained two by two, by means of pairs of steel tendons (10 mm their diameter) joining the adjacent steel bottom flanges. An additional series of FT plates is used in the form of transversal stiffeners and intended to restrain the top steel

Table 2
Examined test scenarios for the 2-side supported panel (central nave path, Fig. 6).

	Occupants		Standing			Walking			Period
	Total p	Density p/m^2	Number	Position	Notes	Number	Position	Notes	
CN#1	1	0.228	–	–	–	1	Centre	Jump	P#1
CN#2	1	0.228	–	–	–	1	Centre	Jump	P#1
CN#3	1	0.228	–	–	–	1	Centre	Jump	P#1
CN#4	1	0.228	–	–	–	1	Centre	Jump	P#1
CN#5	2	0.457	1	Centre	–	1	Overall	Normal Random	P#1
CN#6	3	0.686	1	Centre	–	2	Overall	Normal Random	P#1
CN#7	3	0.686	1	Centre	–	2	Overall	Normal Random	P#1
CN#8	4	0.914	1	Centre	–	3	Overall	Normal Random	P#1
CN#9	4	0.914	3	Centre	–	1	Overall	Normal Random	P#1
CN#10	6	1.372	3	Centre	–	3	Overall	Normal Random	P#1
CN#11	6	1.372	3	Centre	–	3	Overall	Normal Random	P#1
CN#12 CN#13	0	–	–	–	–	–	–	–	P#4
CN#14 to CN#19	1	0.228	–	–	–	1	Overall	Normal Random	P#4
CN#20 to CN#26	2	0.457	–	–	–	2	Overall	Normal Random	P#4

Table 3
Examined test scenarios for the main entrance platform (Fig. 6).

	Occupants		Standing			Walking			Period
	Total p	Density p/m^2	Number	Position	Notes	Number	Position	Notes	
EP#1	1	0.026	–	–	–	1	S#4	Jump	P#1
EP#2	1	0.026	–	–	–	1	Overall	Normal Longitudinal	P#1
EP#3	1	0.026	–	–	–	1	Overall	Normal Random	P#1
EP#4	3	0.078	2	S#4	Mid-span	1	Centre	Jump	P#1
EP#5	3	0.078	2	S#4	Mid-span	1	Overall	Normal Longitudinal	P#1
EP#6	3	0.078	2	S#4	Mid-span	1	Overall	Normal Random	P#1
EP#7 and EP#8	3	0.078	1	S#4	Lateral	2	Overall	Normal Longitudinal Synchronized	P#1
EP#9	3	0.078	1	S#4	Lateral	2	Overall	Normal Longitudinal Crossed	P#1
EP#10	4	0.104	1	S#4	Lateral	3	Overall	Normal Longitudinal Synchronized	P#1
EP#11	5	0.130	1	S#4	Lateral	4	Overall	Normal Longitudinal Synchronized	P#1
EP#12	8	0.208	2	S#4	Lateral	3 + 2+1	Overall	Normal Random	P#1
EP#13	2	0.052	1	S#4	Lateral	1	Overall	Normal Random	P#2
EP#14	3	0.078	1	S#4	Lateral	2	Overall	Normal Random	P#2
EP#15	6	0.156	1	S#4	Lateral	5	Overall	Normal Random	P#2
EP#16	2	0.052	1	S#7	Lateral	1	S#6, S#7	Normal Random	P#3
EP#17	2	0.052	1	S#7	Lateral	1	S#6, S#7	Normal Random	P#3
EP#18	2	0.052	1	S#7	Lateral	1	S#6, S#7	Jump	P#3
EP#19	2	0.052	1	S#7	Lateral	1	S#6, S#7	Consistent Random	P#3
EP#20 and EP#21	1	0.026	1	S#7	Corner	–	–	–	P#4
EP#22 and EP#23	2	0.052	1	S#7	Corner	1	Overall	Normal Random	P#4
EP#24 and EP#25	3	0.078	1	S#7	Corner	2	Overall	Normal Random	P#4

flanges of adjacent girders (Fig. 5(d)). Bespoke steel restraints (Fig. 5 (e)), are finally used to behave as ideal hinges at the girders ends.

4. Experimental methods

The experimental measurements were collected during several periods of the year, in order to capture any possible effect due to variations in the reference temperature and humidity. Besides the case-study footbridge can be rationally recognized as an "indoor" pedestrian system, the Basilica monument is characterized by non-controlled ambient conditions. Accordingly, it was shown in Refs. [16,58,59] that PVB layers in use can be highly sensitive to several aspects, thus further affect the experimental estimation of HSI phenomena.

A total of four test campaigns was taken into account (Table 1). Among them, the test instruments and methods were kept fix.

The acceleration measurements were performed using the Micro Electro-Mechanical System (MEMS) triaxial accelerometers prototyped in Ref. [60].

Given the maximum span of the 2-side supported panels (1.65 m wide × 2.65 m long, with $L_0 = 2.55$ the bending span) and the main entrance platform, as well as some restrictions for the on-site experimental measurements, a total number of six accelerometers was used for each test repetition (see for example the #n sensors of Fig. 6(a)). Their position was aimed at properly capture the fundamental vibration frequencies. The test setup was optimized and refined based on FE models carried out in accordance with [16], and aimed at preliminary capturing the first vibration modes of the examined systems (Fig. 7).

Output-only test data were collected in periods according to Table 1. Careful consideration was spent for the experimental analysis of various HSI scenarios of technical interest for the examined footbridge (Fig. 6). These scenarios of imposed random vibrations involved up to 30 adults (≈80 kg their average weight), and up to 50 loading configurations for the central nave and main entrance systems.

A summary of the examined walking conditions is presented in Tables 2 and 3. There, the setup features are grouped by period of the year (P#n) for each campaign of measurements, and then listed by total number of occupants p. A further distinction of test scenarios is provided in terms of number of standing or walking human bodies, as well as qualitative movement features.

The testing scenarios listed in Tables 2 and 3, more in detail, were detected so as to reproduce the typical operational conditions for the case-study footbridge, i.e. with visitors walking on the suspension system, moving by small groups, standing on the structure to admire the floor mosaics, etc. Accordingly, it is recognized that the same structural system under different operational/ambient conditions would reflect in other comfort limits/dynamic behaviours.

Globally, the test measurements involved a variable number of male and female subjects, that were asked to walk back and forth (or randomly) along the monitored footbridge. The step frequency of normal or consistent walks was in the range of 2–3 Hz, for all the tested

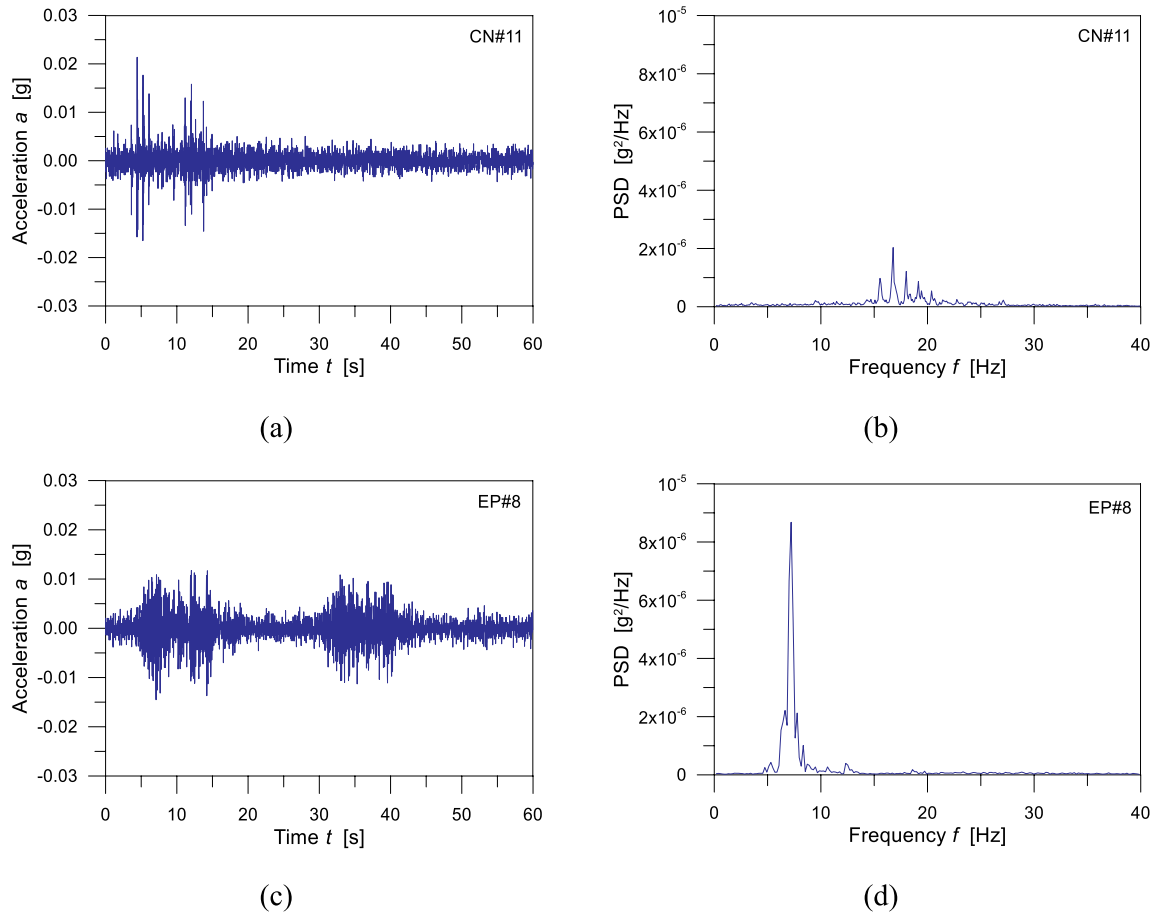

Fig. 8. Examples of vibration measurements (with a focus on vertical component of accelerations). (a)–(c) Acceleration-time history and (b)–(d) Power Spectral Density functions (PSD) for the CN#11 and EP#8 scenarios.

scenarios. In some cases, additional measurements were carried out with a single occupant standing on the structure, and imposing an impulsive vibration in-place jump (see for example CN#1-to-#4 in Table 2). Even not necessarily associated to real operational conditions, these configurations were deliberately reproduced for comparative purposes only.

Special care was hence spent for the analysis of dynamic effects due to:

- synchronized or unsynchronized motion of the occupants (for $p \geq 2$),
- normal or consistent walk of the occupants,
- regular (i.e., longitudinal, back and worth) or irregular (i.e., random) walking path for each occupant.

5. Discussion of test results

The acceleration data were recorded with a sampling frequency of 128 Hz, and the typical record was characterized by a duration of 2 min. Tri-axial MEMS allowed to collect acceleration data for the vertical and horizontal (longitudinal and transversal) directions. Given the intrinsic features of the case-study footbridge, the horizontal acceleration components were found to be negligible, compared to the vertical measurements. An example of collected acceleration records and corresponding Power Spectral Density functions (PSD) is proposed in Fig. 8. The experimental data were post-processed and analysed via the SMIT Toolsuite [61], based on the ERA-OKID-OO approach [62,63]. The fundamental frequency f and damping ξ were hence estimated for all the selected test scenarios.

5.1. Central nave path

The 2-side supported glass panel belonging to the central nave path was first taken into account. Based on previous studies reported in Ref. [16], the selected system in the empty configuration was found to be characterized by a total mass $M_{glass} = 460$ kg (LG+AN layers), with $f_{es} = 15.1$Hz the mean fundamental frequency and $\xi_{es} = 1.15\%$ the corresponding modal damping.

5.1.1. Maximum accelerations and human comfort

At a preliminary stage, the acceleration peaks were assessed with respect to conventional limits and serviceability approaches in use for pedestrian structures composed of traditional constructional materials. According to literature documents (see for example the AISC Design Guide 11 [44]), for example, the maximum acceleration peaks a_{max} (expressed as % value of the acceleration gravity g) for pedestrian systems should not exceed the value $a_{lim} = 5\%$g (“outdoor” footbridges in service conditions). A minimum $a_{lim} = 1.5\%$g is recommended for “indoor” pedestrian systems, as in the current study.

Certainly, literature analytical approaches and limit values for the vibration serviceability assessment of pedestrian structures should be carefully applied to different structural typologies. This is especially the case of glass pedestrian systems, whose dynamic parameters (and their correlation/sensitivity to pedestrian loads) cannot be compared to structures composed of traditional materials. However, specific performance parameters and indicators are currently not available for glass systems. In addition, in the case of glass, it is also recognized that a certain comfort level estimate could be affected by acceleration peaks as well as subjective feelings of the occupants (see for example [59]). In

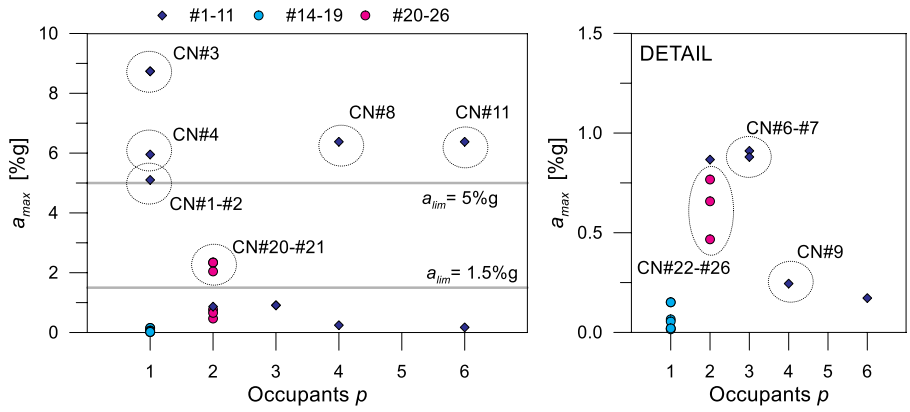

Fig. 9. Recorded acceleration peaks (in %g), for the CN# test scenarios, as a function of the total number of occupants. In evidence, the limit values provided by the AISC Design Guide 11 [44].

this regard, the current experimental investigation represents a first step towards the detailed analysis and assessment of in-service glass pedestrian systems.

In Fig. 9, it can be shown that the examined 2-side supported panel can be associated to a mean acceleration peak of ≈2.3% g, hence representing for the AISC Design Guide 11 a full satisfaction of vibration comfort for outdoor structures. This is not in line with indoor requirements of the same document, however, given that the limit is exceeded for most of the tested scenarios. The limit condition is hardly satisfied even in presence of a limited number of occupants ($p = 2$), due to the intrinsic structure flexibility. In this context, a relatively high scatter can be also noticed between the collected data, with peaks up to 8.8%g. Such an experimental outcome, however, was mostly associated to/justified by test scenarios with consistent/impulsive imposed vibrations ($p = 1$ with in-place jump of the occupant), but also to scenarios with random/normal walk and a relatively high occupation density ($p =$ 4 or 6, mixed walking/standing occupants).

It is worth mentioning that the actual frequency of the empty structure ($f_{es} = 15.1$Hz) was found to be relatively low (down to −30%), compared to the "design" configuration of the system ($f_{es,design} =$ 19.5Hz). Based on [16], such a marked frequency decrease resulted to derive from the stiffness degradation of PVB foils (due to long term phenomena and unfavourable ambient conditions), compared to their nominal mechanical stiffness (with G_{int}≈1.35 MPa the calculated equivalent shear modulus, in place of an expected value of ≈8 MPa for room temperature and short term loads, see also [6,7,16,58]).

As far as the simplified serviceability criterion recommended in the AISC Design Guide 11 [44] for footbridges/floors supported by steel members is taken into account, the vibration verification can be carried out by comparing the expected peak acceleration ($100 \times a_{max}/g$) with the limit acceleration values previously recalled, that is:

$$100 \cdot \frac{a_{max}}{g} = \frac{P_o exp(-0.35 \cdot f)}{\beta W} \leq 100 \cdot \frac{a_{lim}}{g} \tag{5}$$

According to [11], P_0 is a constant force representing the excitation (0.41 kN for "indoor footbridges" and 0.29 kN for "churches, residences, offices"), f the fundamental frequency (in Hz), β the modal damping ratio (equal to 0.01 for "indoor footbridges", or 0.02 for "churches") and W the effective weight (value in kN) that is supported by the steel beam, joists of girder panes (as applicable).

For the examined 2-side supported panel, given $f = f_{es} = 15.1$Hz and W= M_{glass}, the inequality of Eq. (5) would result in unsatisfactory vibrational performances, with a maximum acceleration peak up to 4.59%g > 1.5%g for indoor footbridges, with ≈3.15 the exceedance ratio). Even considering the structure as a pedestrian system "within a church", Eq. (5) would manifest an unsatisfactory acceleration ratio (1.62%g > 0.5%g, that is ≈3.24 the exceedance ratio). This behaviour is further analysed in Fig. 10, where it is possible to notice that the original "design" dynamic performance of the structure fully satisfy the vibration serviceability requirements (1.06%g < 1.5% for indoor footbridges and 0.37%g < 0.5%g for church requirements). Otherwise, as far as the PVB stiffness decreases, the f also decreases and leads to unfavourable estimates, hence suggesting the key role of continuous maintenance interventions and monitoring programmes for vulnerable systems like glass structures.

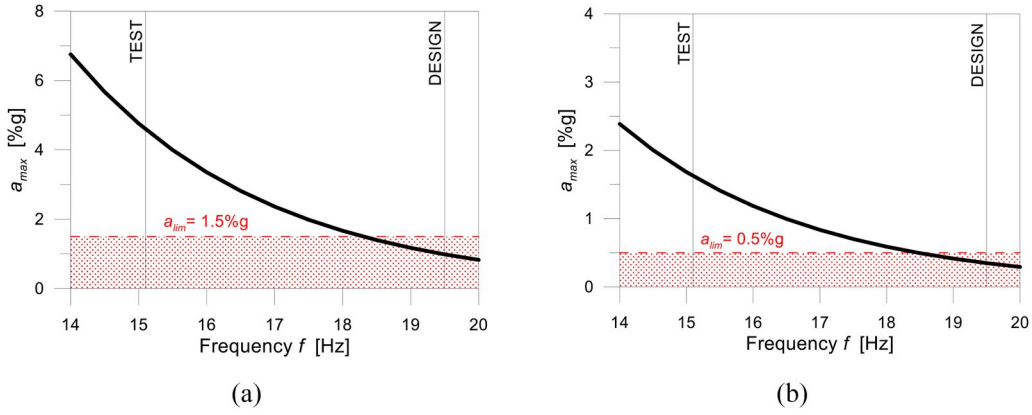

Fig. 10. Vibration serviceability assessment for the 2-side supported panel, based on the AISC Design Guide 11 provisions [44] and Eq. (5). (a) Indoor footbridge and (b) church requirements.

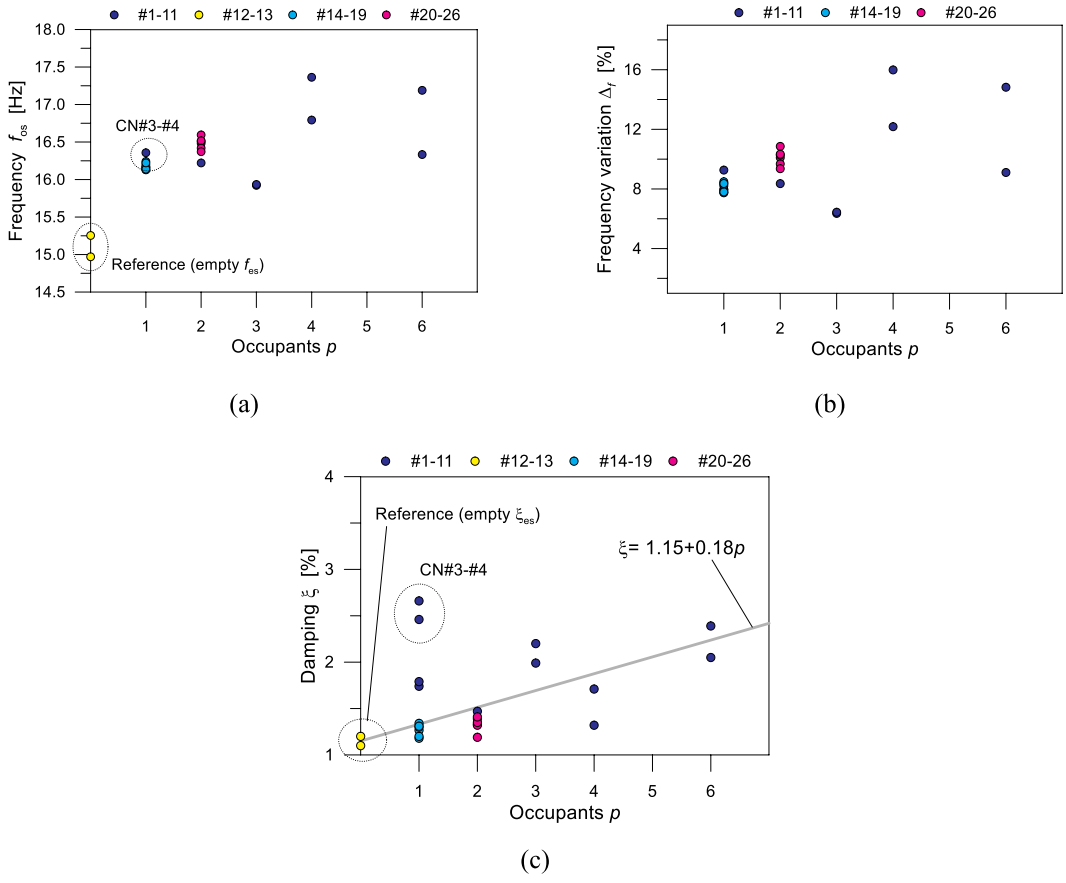

Fig. 11. Variation of (a) fundamental frequency, (b) frequency scatter and (c) damping for the 2-side supported plate, as a function of the total number of occupants.

5.1.2. Dynamic performance and occupants

Given the available test scenarios of Table 2, the mean estimations of CN#12 and CN#13 configurations (empty structure) were taken into account as a reference condition, to investigate the frequency and damping variation while increasing the number of standing/walking human bodies. As far as all the dynamic measurements are taken into account for the single LG + AN panel in bending, see Fig. 11(a) and (c), an increase of fundamental frequency $f_{os} > f_{es}$ and modal damping $\xi_{os} > \xi_{es}$ with p was generally observed. Based on Eq. (5) and Fig. 10, it is worth mentioning that a frequency increase may also result in a positive satisfaction of vibration serviceability requirements.

For reliable investigations, however, multiple features and influencing parameters for the occupants (i.e., number, mass, movement type) should be taken into account. Another key aspect for glass structures – as recalled in Section 2 – is represented by ambient testing conditions (and their effects on PVB properties). The test measurements were carried out between late November 2017 and early Spring 2019, one and half years apart, with variations of mean temperature and humidity (Table 1). Accordingly, for P#1 measurements, possible ambient effects could be expected in a further decrease of PVB stiffness, due to:

- an higher mean temperature during the P#1 experiments (13.2 °C instead of 6.5°),
- a longer life time of the tested panel, within the P#1 scenarios, with increased ageing effects

In Fig. 11(b), frequency scatter values are calculated as:

$$\Delta_f = 100 \cdot \frac{(f_{os} - f_{es})}{f_{es}} \tag{6}$$

A maximum estimate in the order of $\Delta_f = +15$–18% was obtained ($p = 4$), compared to the empty structure. For $p > 0$, moreover, it can be perceived that f_{os} predictions are slightly affected by ambient conditions and time (i.e., P#1 vs. P#4 estimates). When $p = 1$, even in presence of a relatively wide range of imposed accelerations (see Fig. 9), the calculated frequency scatter is in fact +8.08% (P#1) and +8.34% (P#4).

For $p > 1$ (P#1), a frequency increase up to $\Delta_f = +14\%$ was calculated. Given the identical ambient conditions for the full P#1 campaign, such a result is mostly related to the combined number of standing/walking people. This effect is also emphasized in Table 4, where the mean experimental estimates Δ_f (i.e., average results grouped by p) are not proportional to p. The added mass ratio R_M is also reported in Table 4, with:

$$R_M = \frac{M_p}{M_{glass}} \tag{7}$$

Table 4
Frequency (mean % value) and damping (mean % value) variations for the 2-side supported panel (P#1 scenarios), when changing the number of occupants, with respect to the empty structure.

Occupants p			Loading condition (mean)		Frequency variation Δ_f [%]	Damping ξ [%]
Total	Standing	Walking	R_M (Eq. (7))	a_{max} [%g]		
1	0	1	0.182	7.13	+8.34	2.163
2	1	1	0.332	0.87	+8.35	1.470
3	2	1	0.546	0.91	+6.39	2.095
4	1	3	0.964	3.30	+14.08	1.515
6	3	3	1.350	3.27	+11.96	2.220

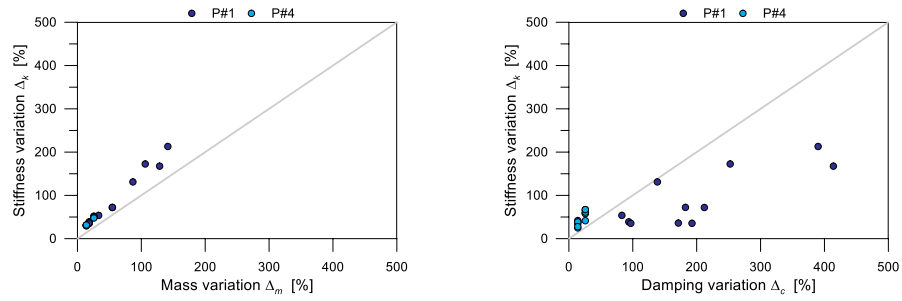

Fig. 12. Sensitivity of (a) modal mass and (b) damping estimates of the occupied structure, with respect to the modal stiffness, for all the CN#*n* scenarios.

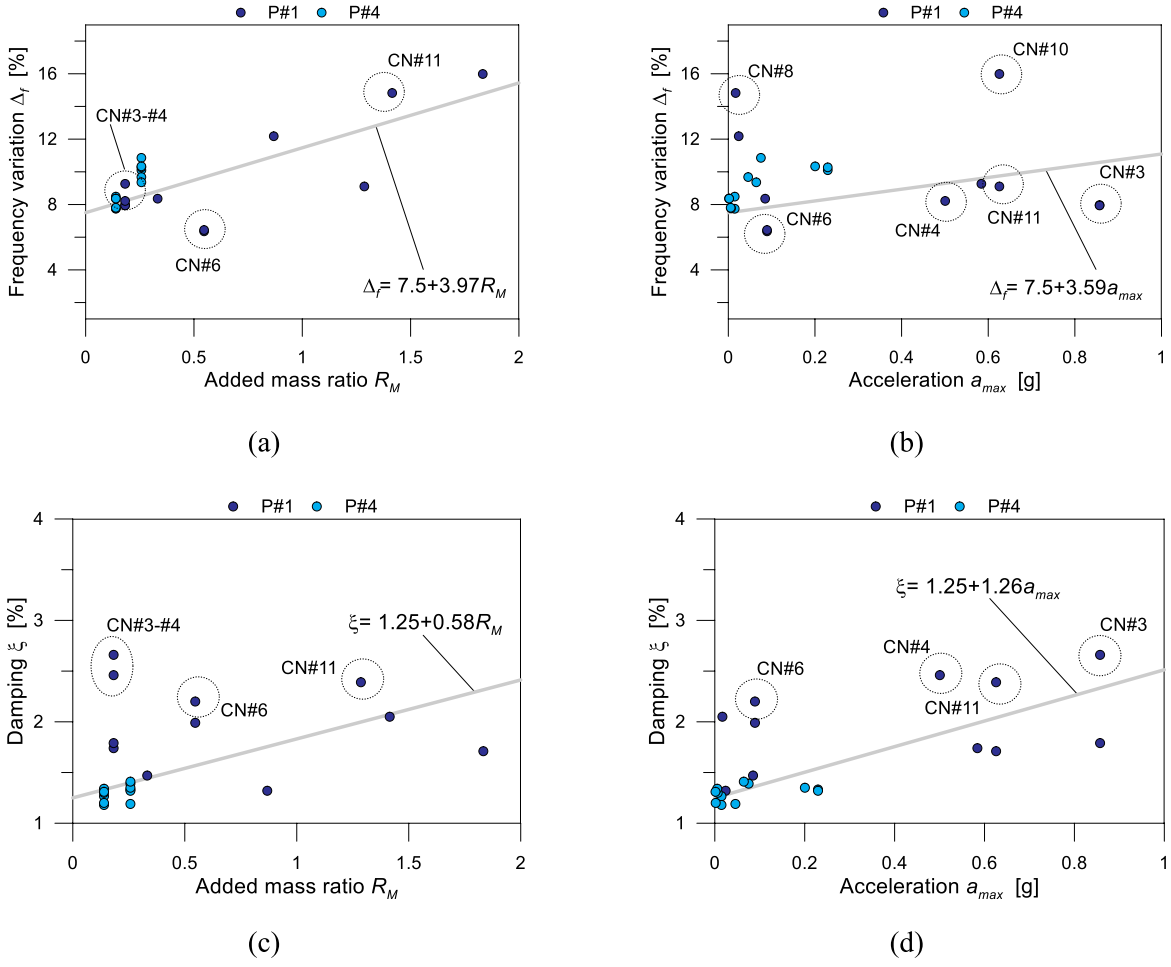

Fig. 13. Variation of (a)–(b) fundamental frequency and (c)–(d) damping, as a function of the added mass ratio and imposed acceleration peak.

denoting the ratio between the total mass of occupants M_p and M_{glass}.

Based on the overall dimensions of the examined glass panel (1.65 × 2.65 m^2) and on the tested configurations (Table 2), it can be reasonably concluded that a frequency increase up to $\Delta_f = +15$–20% could be expected for the occupied structure. However, beside such a marked frequency increase, the human comfort limit condition of Fig. 10 would be in any case not satisfied (≈1.6%g > 1.5%g for the indoor footbridge), hence suggesting retrofit interventions.

In terms of damping predictions (ξ_{os}), see Fig. 11(c) and Table 4, the presence of standing/walking people increased up to two times the empty performance (ξ_{es} = 1.15%). These variations, however, include variable movements and also in-place jumps characterized by large/impulsive imposed accelerations, and thus more pronounced damping phenomena.

As far as more detailed calculation approaches are not available, and given the loading configurations herein explored, a simple (ξ_{os}, p) linear correlation could be taken into account for preliminary estimates and in-service monitoring investigations of the 2-side supported system, see Fig. 11(c).

5.1.3. *Modal properties of the occupied system*

In Fig. 12, the percentage variations of modal parameters of the structure are proposed, with evidence of mass-stiffness and damping-

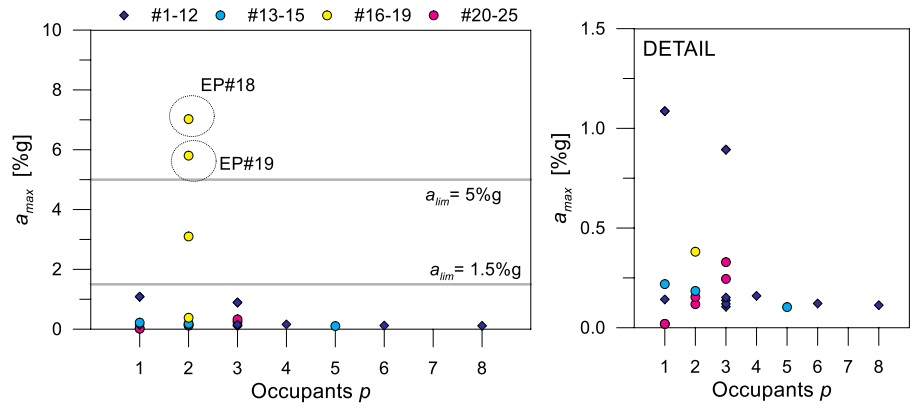

Fig. 14. Recorded acceleration peaks (in %g), for the EP#n test scenarios, as a function of the total number of occupants. In evidence, the limit values provided by the AISC Design Guide 11 [44].

stiffness relationships. The percentage variations are calculated – for all the CN#n scenarios of Table 2 – based on the collected test measurements and in accordance with Eqs. (3) and (4). Test data are grouped by testing period (P#1, P#4).

Generally, it can be seen in Fig. 12(a) that f_{os} is mostly related to a more pronounced stiffness variation. The trend of collected data is roughly linear, with ≈1.88 the mean k_{os}-to-m_{os} variation ratio (up to a maximum of ≈2.28). Conversely, a damping increase – in absolute terms – up to two times the corresponding stiffness can be noticed in Fig. 12 (b). The mean c_{os}-to-k_{os} variation ratio was calculated in ≈1.89, with maximum peaks up to ≈5.4 (for test scenarios characterized by consistent/impulsive human-induced vibrations).

Even from relatively simple OMA dynamic estimates, useful feedback can be derived for drawing considerations of practical use, and find a correlation between the dynamic properties of the system and several operational conditions of technical interest. Such an approach can be useful especially for long-term monitoring purposes.

In Fig. 13, test predictions for the 2-side supported panel are reported as a function of the added mass ratio R_M (Eq. (7)) and imposed acceleration $a_{\max}$ (peak value (in g) for each scenario). All the estimates are grouped by period (P#1 and P#4, according to Table 2).

For the explored configurations, see Fig. 13(a), a mostly linear dependency can be noticed for the frequency variation, with respect to the mass of the occupied structure. Roughly scattered frequency data can indeed be noticed in terms of acceleration peak (Fig. 13(b)). Regarding damping, the structural, material and aeroelastic terms composing the total experimental calculations were found to depend mostly linearly from the acceleration peak (Fig. 13(d)). Such a finding, in this context, follows and extends the preliminary observations reported in Ref. [20] for simple glass members, with the additional influencing parameter represented by the combined effects of standing/human bodies. Major scatter of frequency and damping estimates were generally observed, in Fig. 12, for specific loading conditions (i.e., $p = 1$ with limited R_M but impulsive motion). Finally, given the P#1 or P#4 period (Table 1), no direct correlation was generally found with frequency and damping estimates.

5.2. Main entrance platform

The main entrance suspension platform experimental predictions were then investigated in detail. Compared to the 2-side supported panel of Section 5.1, the total (LG + AN) mass of the pedestrian slab can be calculated in M_{glass}≈4020 kg (for up to ≈40 square meters of covered surface). Such a mass estimate can be assumed as well representative of the mass sustained by steel/glass girders (i.e., for simplified vibration checks according to Ref. [44]). However, this value disregards the contribution of girders, framing members and the steel-glass handrails, which can have also a relevant role on the overall dynamic estimates.

The fundamental frequency of the platform system (with $p = 1$, standing on the structure, with $R_M = 1.7\%$) was experimentally predicted in in $f_{es} = 7.28$Hz, with $\xi_{es} = 1.4\%$ the corresponding modal damping.

5.2.1. Maximum accelerations and human comfort

Compared to the 2-side supported panel, even more critical performances were generally detected for the main entrance platform, as a direct effect of the structural complexity of the system, and of multiple contact interactions between the load-bearing members.

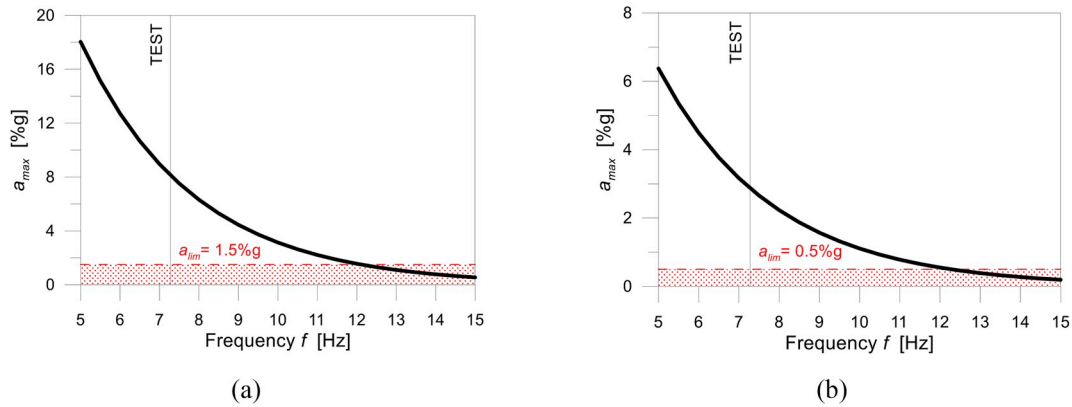

Fig. 15. Vibration serviceability assessment for the main entrance platform, based on the AISC Design Guide 11 provisions [44] and Eq. (5). (a) Indoor footbridge and (b) church requirements.

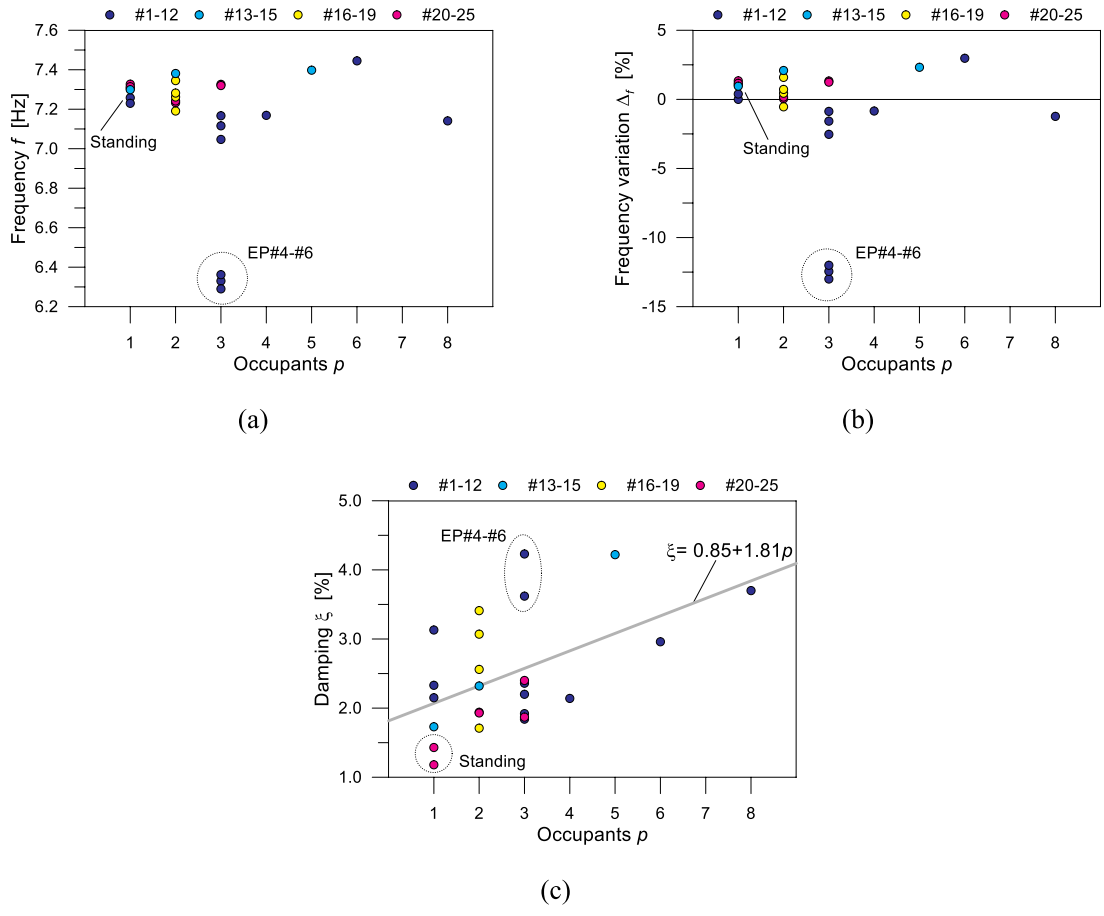

Fig. 16. Variation of (a) fundamental frequency, (b) frequency scatter and (c) damping for the main entrance suspension platform, as a function of the total number of occupants.

While the mean acceleration peak was in fact found to satisfy the 1.5%g limit for indoor structures (0.96%g the average value from the experiments, with maximum peaks up to ≈7%g, see Fig. 14), the vibration serviceability verification according to Ref. [44] and Eq. (5) resulted in any case in unfavourable estimates, see Fig. 15 (with W=M_{glass} and $f = 7.28$Hz).

More in detail, the platform vibration performance was found to be even more unfavourable with respect to the 2-side supported panel, with 8.12%g > 1.5%g for the indoor footbridge configuration (≈5.4 the exceedance ratio) and 2.86%g > 0.5%g according to church requirements (≈5.7 the ratio).

Compared to the 2-side supported panel (see Section 5.1 and [16]), however, the "design" performances for the composite platform are not available. Accordingly, the actual performance can be reasonably expected to derive from multiple key factors (i.e., PVB degradation, etc.), hence suggesting the need of more accurate studies and interventions.

5.2.2. Dynamic performance and occupants

For the overall platform, the sensitivity of frequency predictions to the testing period (P#1 to P#4) or movement features for the occupants (i.e., resting position, normal walk) was found to be negligible (see Fig. 16(a) and (b)). Within the full programme, the added mass ratio R_M was calculated via Eq. (7) in the range from 0.017 ($p = 1$) up to 0.137 (for $p = 8$). In most of the cases - given the global dimensions and the actual boundaries of the platform - stable frequency estimates were generally observed also for $p > 1$ - with respect to the 2-side supported plate. The increase of p was found to manifest in a frequency variation up to $\Delta_f = +2.5\%$ the reference value.

However, the experimental setups also highlighted some possible criticalities that should be properly assessed, and namely a marked decrease of the reference vibration frequency for the overall system. Such an outcome was observed in a limited number of test setups (see the EP#4-to-#6 features in Table 3), with a frequency reduction down to $\Delta_f = -15\%$ (corresponding to $f_{os} = 6.32$Hz).

The EP#4-EP#6 configurations, more in detail, were characterized by two occupants standing in the mid-span region of the slab (S#4 sector and G2-G3 girders, in accordance with Fig. 6(c)), that is where the maximum bending effects are expected for the structure under service loads. Similar trends – even with a less pronounced frequency variation – were observed also for the suspension platform with up to $p = 8$ (EP#12, with 2 standing adults in the central region of the slab and 6 walking randomly with unsynchronized motion on the slab). In the latter case, it was found that $f_{os} = 7.14$Hz (that is $\Delta_f = -1.25\%$, with $R_M = 0.137$).

For the EP#4-EP#6 scenarios, in this regard, the vibration serviceability inequality of Eq. (5) would result in a 7.8–8.4 exceedance ratio, with comfort of the occupants hardly satisfied.

As far as the main platform estimates are considered in terms of damping, see Fig. 16(c), the observed trend was a general damping increase with p. Given that the damping estimates are highly sensitive to p but especially to the movement features (i.e., Fig. 1), the experimental predictions resulted in close correlation with past studies on vibrating glass systems. The damping coefficient for the platform with a $p = 1$ (standing) was calculated in $\xi_{os} = 1.3\%$ that slightly exceeds the 2-side supported system predictions ($\xi_{es} = 1.15\%$) and agrees with [20]. As far as a single occupant at mid-span was asked to jump in-place, the damping estimate increased up to 3.2% (Fig. 16(c)), given the amplitude and impulsive nature of imposed vibrations. Given the geometrical and

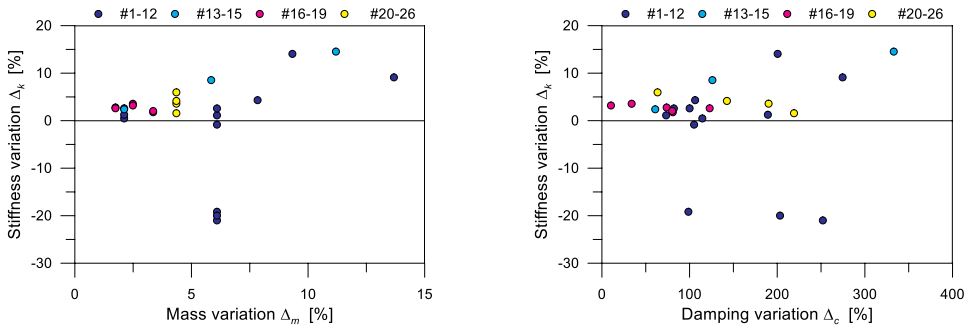

Fig. 17. Sensitivity of (a) mass and (b) damping variation estimates of the occupied structure, with respect to the modal stiffness of the system, for all the EP#*n* testing scenarios.

mechanical complexity of the platform structure, however, it can be seen that – in absence of more detailed calculation methods - damping predictions can be roughly estimated via a linear relationship.

5.2.3. Modal properties of the occupied system

In conclusion, according to Eqs. (3) and (4), the sensitivity of mass, stiffness, damping variations with respect to the imposed human-induced loads was taken into account. The so collected data are reported in Fig. 16. As shown, the k_{os} was found to increase more than proportionally to the corresponding m_{os} values. On the other hand, the k_{os} was observed to increase faster with respect to the c_{os}, and such a finding should be further explored. For both Fig. 17(a) and (b), finally, mostly scattered trends can be noticed, for mass-stiffness and damping-stiffness correlations. Such an outcome is in contrast with the test estimates of the 2-side supported specimen, but at the same time can be reasonably justified by the geometrical and mechanical features of the platform structure.

6. Summary and conclusions

Structural glass is recognized to act, in modern buildings, as a constructional material with load-bearing capacities. The vulnerability of glass structures can be minimized based on rigid design assumptions to satisfy, ensuring huge consequences for the occupants in the case of accidental/extreme events, or limited comfort in service conditions. Specific criticalities, in this regard, may derive from vibration requirements in service condition, due to the typically high slenderness of glazed structural components, as well as to the use of materials/restraint details that may mechanically degrade with time/temperature/humidity.

In this paper, based on Operational Modal Analysis (OMA) techniques, the dynamic performance of an in-service suspension glass structure was experimentally investigated. Given the location of the case-study system (monumental church) and its typical use (i.e., loading scenarios characterized by mixed walking/standing occupants), a wide range of test setup configurations was taken into account, so to assess the sensitivity of the structure of Human-Structure Interaction (HSI) phenomena. The experimental investigation was specifically focused on two different regions, i.e., an independent, 2-side supported glass panel with a beam-like behaviour (with intermediate, unilateral point-supports), and a composite suspension platform system. In the latter case, the object of investigation was still characterized by a global beam-like behaviour, but the overall assembly was obtained as the combination of multiple glass panels and frame steel members offering a continuous linear support along the four edges of each plate. Based on selected walking traffic configurations, in particular, it was shown that the fundamental vibration frequency of the empty or occupied structure is strictly related to the actual boundary conditions (i.e., 2-side supported independent plates or suspension platform system). Moreover, the occupation density and movement features can significantly affect the vibration properties of the empty system object of analysis, with important variations for both the corresponding vibration frequency and damping coefficients. As far as HSI phenomena are related to the dynamic properties of the structure and the occupants, major sensitivity was observed for the 2-side supported plates (with up to +16% for the vibration frequency, compared to the empty structure). The suspension platform, in this sense, still emphasized an increase of fundamental frequency with occupants, but up to +5% the empty structure.

In general, such a series of experimental observations can be thus extended to pedestrian glass structures with different mechanical features. Compared to other constructional typologies for pedestrian structures, glass systems are in fact characterized by high span-to-thickness ratios, thus relatively small structural mass with respect to the occupants. HSI phenomena should be hence properly investigated. As far as the mechanical properties of the materials in use for glass structures can modify and suffer for degradation with time/temperature/ambient conditions, moreover, dedicated studies and calculation methods should be further explored for safe design purposes.

Declaration of competing interest

The authors declare that they have no known competing financial interests or personal relationships that could have appeared to influence the work reported in this paper.

CRediT authorship contribution statement

Chiara Bedon: Data curation, Writing - original draft, Writing - review & editing.

Acknowledgements

The So.Co.Ba. Foundation ("Società per la conservazione della Basilica") is gratefully acknowledged for facilitating the experimental measurements.

Appendix A. Supplementary data

Supplementary data to this article can be found online at https://doi.org/10.1016/j.jobe.2020.101195.

References

[1] M. Haldimann, A. Luible, M. Overend, Structural Use of Glass, IABSE, Zurich, 2008, ISBN 978-3-85748-119-2. CH.
[2] J. Wurm, Glass Structures: Design and Construction of Self-Supporting Skins, Springer Science, 2007. EAN: 9783764376086.

[3] R. Zarnic, G. Tsionis, E. Gutierrez, A. Pinto, M. Geradin, S. Dimova, Purpose and Justification for New Design Standards Regarding the Use of Glass Products in Civil Engineering Works, 2007. EUR 22856 EN, ISSN: 1018-5593.
[4] M. Badalassi, L. Biolzi, G. Royer-Carfagni, W. Salvatore, Safety factors for the structural design of glass, Constr. Build. Mater. 55 (2014) 114–127.
[5] F. Pariafsai, A review of design considerations in glass buildings, Frontiers of Architectural Research 5 (2) (2016) 171–193.
[6] M. Feldmann, R. Kasper, et al., Guidance for European structural design of glass components – support to the implementation, harmonization and further development of the eurocodes, in: Dimova, Feldmann Pinto, Denton (Eds.), Report EUR 26439–Joint Research Centre-Institute for the Protection and Security of the Citizen, 2014, https://doi.org/10.2788/5523.
[7] CNR-DT 210/2013, Istruzioni per la Progettazione. l'Esecuzione ed il Controllo di Costruzioni con Elementi Strutturali in Vetro (in Italian), National Research Council (CNR), Roma, Italy, 2013. www.cnr.it.
[8] L. Biolzi, A. Bonati, S. Cattaneo, Laminated glass cantilevered plates under static and impact loading, Adv. Civ. Eng. 2018 (2018), https://doi.org/10.1155/2018/7874618. Article ID 7874618.
[9] C. Bedon, R. Kalamar, M. Eliasova, Low velocity impact performance investigation on square hollow glass columns via full-scale experiments and Finite Element analyses, Compos. Struct. 182 (2017) 311–325.
[10] R.C. Bradt, The fractography and crack patterns of broken glass, J. Fail. Anal. Prev. 11 (2) (2011) 79–96.
[11] F.A. Veer, T. Bristogianni, G. Baardolf, A case study of apparently spontaneous fracture, Glass Structures & Engineering 3 (1) (2018) 109–117.
[12] M. Corradi, E. Speranzini, Post-cracking capacity of glass beams reinforced with steel fibers, Materials 12 (2) (2019) 231, https://doi.org/10.3390/ma12020231.
[13] X. Zhang, C. Bedon, Vulnerability and protection of glass windows and facades under blast: experiments, methods and current trends, International Journal of Structural Glass and Advanced Materials Research 1 (2) (2017) 10–23, https://doi.org/10.3844/sgamrsp.2017.10.23.
[14] H. Dotan, Zhangjiajie grand canyon glass bridge, in: Proceedings of Challenging Glass 5 – Conference on Architectural and Structural Applications of Glass, 2016, ISBN 978-90-825-2680-6.
[15] G. Royer Carfagni, M. Silvestri, A proposal for an arch footbridge in Venice made of structural glass masonry, Eng. Struct. 29 (2007) 3015–3025.
[16] C. Bedon, Diagnostic analysis and dynamic identification of a glass suspension footbridge via on-site vibration experiments and FE numerical modelling, Compos. Struct. 216 (2019) 366–378.
[17] N. Baldassini, Hidden and expressed geometry of glass, in: Bos, Louter, Veer (Eds.), Proceedings of Challenging Glass – Conference on Architectural and Structural Applications of Glass, IOS Press, 2008.
[18] P. Lenk, H. Lambert, Challenges in the design, fabrication and installation of glass structures comprising of super jumbo glass sheets, in: Louter Bos, Veer Nijsse (Eds.), Proceedings of Challenging Glass 3 – Conference on Architectural and Structural Applications of Glass, 2012, https://doi.org/10.3233/978-1-61499-061-1-101.
[19] L. Andreozzi, S. Briccoli Bati, M. Fagone, G. Ranocchiai, F. Zulli, Weathering action on thermo-viscoelastic properties of polymer interlayers for laminated glass, Constr. Build. Mater. 98 (2015) 757–766.
[20] C. Bedon, M. Fasan, C. Amadio, Vibration analysis and dynamic characterisation of structural glass elements with different restraints based on Operational Modal Analysis, Buildings 9 (1) (2019), https://doi.org/10.3390/buildings9010013.
[21] E. Shahabpoor, A. Pavic, V. Racic, Interaction between walking humans and structures in vertical direction: a literature review, Shock Vib. 2016 (2016), https://doi.org/10.1155/2016/3430285. Article ID 3430285.
[22] H. Bachmann, W. Ammann, Vibrations in structures induced by man and machines, Structural Engineering Documents 3e (1987). International Association of Bridge and Structural Engineering (IABSE), Zurich, CH.
[23] C.A. Jones, A. Pavic, P. Reynolds, R.E. Harrison, Verification of equivalent mass-spring-damper models for crowd-structure vibration response prediction, Can. J. Civ. Eng. 38 (10) (2011) 1122–1135.
[24] Y. Matsumoto, M.J. Griffin, Dynamic response of the standing human body exposed to vertical vibration: influence of posture and vibration magnitude, J. Sound Vib. 212 (1) (1998) 85–107.
[25] M. Bocian, J. Macdonald, J. Burn, Modelling of self-excited vertical forces on structures due to walking of pedestrians, in: Proceedings of the 8th International Conference on Structural Dynamics, 2011. EURODYN 2011.
[26] B.R. Whittington, D.G. Thelen, A simple mass-spring model with roller feet can induce the ground reactions observed in human walking, J. Biomech. Eng. 131 (1) (2009), 011013, https://doi.org/10.1115/1.3005147.
[27] ABAQUS, Dassault Systémes. ABAQUS Computer Software V. 6.14, 2017. Providence. RI. USA).
[28] R.W. Clough, J. Penzien, Dynamics of Structures, McGraw-Hill, 1993, ISBN 0-07-011394-7.
[29] L. Galuppi, G. Royer-Carfagni, Enhanced Effective Thickness of multi-layered laminated glass, Compos. B Eng. 64 (2014) 202–213.
[30] Y. Koutsawa, E.M. Daya, Static and free vibration analysis of laminated glass beam on viscoelastic supports, Int. J. Solids Struct. 44 (2007) 8735–8750.
[31] F. Pelayo, M. Lopez-Aenlle, Natural frequencies and damping ratios of multi-layered laminated glass beams using a dynamic effective thickness, J. Sandw. Struct. Mater. (2017), https://doi.org/10.1177/1099636217695479.
[32] A. Zemanova, J. Zeman, T. Janda, J. Schmidt, M. Sejnoha, On modal analysis of laminated glass: usability of simplified methods and Enhanced Effective Thickness, Compos. B Eng. 151 (2018) 92–105.
[33] A. Ramos, F. Pelayo, M.J. Lamela, A. Fernandez Canteli, C. Huerta, A. Pacios, Evaluation of damping properties of structural glass panes under impact loading, in: Proceedings of COST Action TU0905 Mid-term Conference on Structural Glass, 2013, ISBN 978-1-138-00044-5.
[34] Q. Feng, L. Fan, L. Huo, G. Song, Vibration reduction of an existing glass window through a viscoelastic material-based retrofit, Appl. Sci. 8 (7) (2018) 1061, https://doi.org/10.3390/app8071061.
[35] C. Bedon, C. Amadio, Numerical assessment of vibration control systems for multi-hazard design and mitigation of glass curtain walls, Journal of Building Engineering 15 (2018) 1–13.
[36] A. Krstic-Furundzic, T. Kosic, J. Terzovic, Architectural aspect of structural glass roof design, in: Louter Belis (Ed.), Proceedings of COST Action TU0905 Mid-term Conference on Structural Glass, Mocibob, 2013, ISBN 978-1-138-00044-5.
[37] J. Cai, Y. Xu, J. Feng, J. Zhang, Design and analysis of a glass roof structure, Struct. Des. Tall Special Build. 22 (2013) 677–686, https://doi.org/10.1002/tal.721.
[38] L. Lauriks, M. de Bow, I. Wouters, Glass in roofs. Study of the 19th century literature on building technology, in: Proceedings of the 1st WTA International PhD Symposium, 2009 (Leuven, Belgium).
[39] L. Galuppi, Transformable curved thin glass greenhouse, International Journal of Structural Glass and Advanced Materials Research 2 (2018) 198–217, https://doi.org/10.3844/sgamrsp.2018.198.217.
[40] J. Bijster, C. Noteboom, M. Eekhout, Glass entrance Van gogh museum amsterdam, Glass Structures & Engineering 1 (1) (2016) 205–231.
[41] D. Honfi, M. Overend, Glass structures – learning from experts, in: Louter Belis (Ed.), Proceedings of COST Action TU0905 Mid-term Conference on Structural Glass, Mocibob, 2013, ISBN 978-1-138-00044-5.
[42] B. Davis, O. Avci, Simplified vibration serviceability evaluation of slender monumental stairs, J. Struct. Eng. 141 (11) (2015), https://doi.org/10.1061/(ASCE)ST.1943-541X.0001256.
[43] ISO 2631-2, Mechanical Vibration and Shock - Evaluation of Human Exposure to Whole-Body Vibration – Part 2: Vibration in Buildings, International Organization for Standardization (ISO), 2003.
[44] T.M. Murray, D.E. Allen, E.E. Ungar, Floor Vibrations Due to Human Activity. Steel Design Guide Series no.11, American Institute of Steel Construction (AISC), Chicago, IL, USA, 2003.
[45] M. Feldmann, C. Heinemeyer, C. Butz, E. Caetano, A. Cunha, F. Galanti, A. Goldack, O. Hechler, S. Hicks, A. Keil, M. Lukic, R. Obiala, M. Schlaich, G. Sedlacek, A. Smith, P. Waarts, Design of Floor Structures for Human Induced Vibrations, 2009, ISBN 978-92-79-14094-5, https://doi.org/10.2788/4640. EUR 24084 EN.
[46] C. Heinemeyer, C. Butz, A. Keil, M. Schlaich, A. Goldack, S. Trometer, M. Lukic, B. Chabrolin, A. Lemaire, P.O. Martin, A. Cunha, E. Caetano, Design of lightweight footbridges for human induced vibrations, EUR 23984 EN (2009), https://doi.org/10.2788/33846. ISBN 978-92-79-13387-9.
[47] S. Zivanovic, A. Pavic, P. Reynolds, Vibration serviceability of footbridges under human-induced excitation: a literature review, J. Sound Vib. 279 (1–2) (2005) 1–74.
[48] Z. Muhammad, P. Reynolds, O. Avci, M. Hussein, Review of pedestrian load models for vibration serviceability assessment of floor structures, Vibrations 2 (1) (2019) 1–24, https://doi.org/10.3390/vibration2010001.
[49] C.A. Jones, P. Reynolds, A. Pavic, Vibration serviceability of stadia structures subjected to dynamic crowd loads: a literature review, J. Sound Vib. 330 (8) (2011) 1531–1566.
[50] Toso Ma, H.M. Gomes, F.T. Silva, R.L. Pimentel, Experimentally fitted biodynamic models for pedestrian-structure interaction in walking situations, Mech. Syst. Signal Process. 72–73 (2016) 590–606.
[51] B.R. Whittington, D.G. Thelen, A simple mass-spring model with roller feet can induce the ground reactions observed in human walking, Journal of Biomechanical Engineering 131 (1) (2009). Article ID 011013.
[52] L. Cao, H. Qi, J. Li, Experimental and numerical studies on the vibration serviceability of fanshaped prestressed concrete floor, Int. J. Distributed Sens. Netw. 14 (8) (2018), https://doi.org/10.1177/1550147718795746.
[53] C.M. Abeysinghe, D.P. Thambiratnam, J.N. Perera, Dynamic performance characteristics of an innovative hybrid composite floor plate system under human-induced loads, Compos. Struct. 96 (2013) 590–600.
[54] L. Cao, H. Qi, J. Li, Experimental and numerical studies on the vibration serviceability of fanshaped prestressed concrete floor, Int. J. Distributed Sens. Netw. 14 (8) (2018), https://doi.org/10.1177/1550147718795746.
[55] J.G.S. da Silva, P.C.G.S. Vellasco, S.A.L. de Andrade, Vibration analysis of orthotropic composite floors for human rhythmic activities, J. Braz. Soc. Mech. Sci. Eng. XXX (1) (2008) 56–65.
[56] G. Busca, A. Cappellini, S. Manzoni, M. Tarabini, M. Vanali, Quantification of changes in modal parameters due to the presence of passive people on a slender structure, J. Sound Vib. 333 (2014) 5641–5652.
[57] M. Setareh, S. Gan, Vibration testing, analysis and human-structure interaction studies of a slender footbridge, J. Perform. Constr. Facil. 32 (2018), https://doi.org/10.1061/(ASCE)CF.1943-5509.0001213, 040018068.
[58] C. Bedon, Issues on the vibration analysis of in-service laminated glass structures: analytical, experimental and numerical investigations on delaminated beams, Appl. Sci. 9 (18) (2019) 3928, https://doi.org/10.3390/app9183928.
[59] C. Bedon, M. Fasan, Reliability of field experiments, analytical methods and pedestrian's perception scales for the vibration serviceability assessment of an in-service glass walkway, Appl. Sci. 9 (9) (2019) 1936, https://doi.org/10.3390/app9091936.
[60] C. Bedon, E. Bergamo, M. Izzi M, S. Noè, Prototyping and validation of MEMS accelerometers for structural health monitoring - the case study of the

pietratagliata cable-stayed bridge, J. Sens. Actuator Netw. 7 (3) (2018) 30, https://doi.org/10.3390/jsan7030030.
[61] SMIT, Structural modal identification toolsuite, Available online (accessed on December 2018), http://smit.atlss.lehigh.edu, 2018.
[62] M. Chang, R.L. Leonard, S.N. Pakzad, SMIT user's Guide. Release 1.0, 2012. Available online, http://smit.atlss.lehigh.edu/wp-content/uploads/2012/07/SMIT-Users-Guide.pdf, 2012.
[63] M. Chang, S.N. Pakzad, Observer kalman filter identification for output-only systems using interactive structural modal identification toolsuite, J. Bridge Eng. 19 (2014), 04014002.